Arch Appl Mech (2011) 81:1607–1620
DOI 10.1007/s00419-011-0505-4

ORIGINAL

Bogdan Rogowski

The mode III cracks emanating from an elliptical hole in the piezo-electro-magneto-elastic materials

Received: 13 July 2010 / Accepted: 22 December 2010 / Published online: 26 February 2011

Abstract The mode III crack problem in a medium possessing coupled electro-magneto-elastic is considered. Two asymmetrical edge cracks emanate from an elliptical hole. Combined stress, electric and magnetic loads are considered. The elliptical hole and cracks are assumed to be either magneto-electrically impermeable or permeable. The closed-form solution for stress, electric and magnetic intensity factors are derived explicitly. Also the solution for energy release rate is given in closed form. The solution is based on the complex variable method combined with the method of conformal mapping. Numerical computations are given to illustrate the effect of variable geometrical and material parameters on stress, electric and magnetic intensity factors and energy release rate.

Keywords Magneto-electro-elastic solid · Complex variable methods · Conformal mapping methods · Stress, electric and magnetic intensity factors · Energy release rate · Exact solution · New shape of crack

1 Introduction

Material possessing magneto-electro-elastic coupling effects have found increasing applications in engineering structures, particularly in "smart" materials and "intelligent" structures. The effects of magneto-electromechanical coupling have been observed in single-phase materials in which simultaneous magnetic and electric ordering coexists and in two-phase composites where the participating phases are piezoelectric and piezomagnetic. These "smart" materials are extensively used as electric packaging, sensors and actuators, magnetic field probes, acoustic and ultrasonic devices, hydrophones and transducers with the responsibility of electro-magneto-mechanical energy conversion. When subjected to mechanical, electrical and magnetic loads in service, these magneto-electro-elastic composites can fail prematurely due to some defects, namely cracks, holes and others, arising during their manufacturing process. Therefore, it is of great importance to study the magneto-electro-elastic interaction and fracture behaviours of magneto-electro-elastic materials.

On the other hand, composites possess some new properties of magneto-electricity with the secondary pyroelectric effects which are not found in single-phase piezoelectric or piezomagnetic materials. In some cases, the magneto-electric effects of piezoelectric/piezomagnetic composites can be obtained by a hundred times larger than that of a single-phase magneto-electric material.

For piezoelectromagnetic ceramics, anti-plane shear cracks are a class of simple crack problems. However, for an anti-plane shear cracks terminating from the edge of elliptical hole in piezo-electro-magneto-elastic ceramics, related studies are absent to the best of the author's knowledge. It is worth noting that for purely elastic media and piezoelectric media with an anti-plane shear crack terminating from the edge of circular hole, these situations have been analysed by many researchers. Wang and Gao [18] studied the mode III fracture problem of edge cracks originating from a circular hole in an infinite piezoelectric solid based on the

B. Rogowski (✉)
Department of Mechanics of Materials, Technical University of Lodz, Al. Politechniki 6, 93-590 Lodz, Poland
E-mail: brogowsk@p.lodz.pl

complex variable method combined with the method of conformal mapping. Explicit and exact expressions for the complex potentials, field intensity factors and energy release rate were presented under the assumption that the surface of the cracks and hole is electrically impermeable. An elliptical cavity in a magneto-electro-elastic solid under an in-plane electromagnetic and/or anti-plane mechanical loading was investigated by [2]. By reducing the cavity to a crack, the extreme cases for an impermeable and a permeable crack were obtained. The crack problems in brittle piezoelectric materials under anti-plane shear loading have attracted much attention in recent years, for example, [3,6,14,15,19,21–23].

Here it is specially noted that the fracture mechanics of magneto-electro-elastic layered or functionally graded materials have attracted much attention and many research papers have been published (see, e.g. [4,5,7,9,16,24] among others).

In this article, the mode III stress, electric and magnetic intensity factors and singularities analysis for edge cracks emanating from an elliptical hole in a piezo-electro-magneto-elastic material is presented. The results presented here contain the previous known solutions as special cases of elastic, piezoelectric, piezomagnetic materials for example. Moreover, new results for magneto-electro-elastic material with cracks are obtained, such as two nonsymmetric or symmetric cracks and a single crack emanating from an elliptical fole, cross-shaped crack, T-shaped crack, and so on. In order to gain better understanding for the theoretical results, numerical computations are given to illustrate the effect of variable geometrical and material parameters on stress, electric and magnetic intensity factors and energy release rate.

2 Basic equations

For a linearly magneto-electro-elastic medium under anti-plane shear coupled with in-plane electrical and magnetical fields, there are only the non-trivial anti-plane displacement w, strain components γ_{xz} and γ_{yz}, stress components τ_{xz} and τ_{yz}, in-plane electric and magnetic potentials φ and ψ, electric field components E_x and E_y, electric displacement components D_x and D_y, magnetic field components H_x and H_y, magnetic induction components B_x and B_y with all field quantities being only the functions of coordinates x and y.

The generalized strain–displacement relations have the form

$$\gamma_{\alpha z} = w_{,\alpha}, \quad E_\alpha = -\varphi_{,\alpha}, \quad H_\alpha = -\psi_{,\alpha} \tag{1}$$

where $\alpha = x, y$ and $w_{,\alpha} = \partial w/\partial\alpha$.

For linearly magneto-electro-elastic medium, the coupled constitutive relation can be written in the form

$$[\tau_{\alpha z}, D_\alpha, B_\alpha]^T = \mathbf{C}[\gamma_{\alpha z}, -E_\alpha, -H_\alpha]^T \tag{2}$$

where the superscript T denotes the transpose of a matrix and

$$\mathbf{C} = \begin{bmatrix} c_{44} & e_{15} & q_{15} \\ e_{15} & -\varepsilon_{11} & -d_{11} \\ q_{15} & -d_{11} & -\mu_{11} \end{bmatrix} \tag{3}$$

where c_{44} is the shear modulus along the z-direction which is perpendicular to the isotropic plane (x, y), ε_{11} and μ_{11} are dielectric permittivity and magnetic permeability coefficients, respectively, e_{15}, q_{15} and d_{11} are piezoelectric, piezomagnetic and magneto-electric coefficients, respectively. The medium is poled along the z-direction.

The equilibrium equation, the charge and current conservation equations, in the absence of the body force, electric and magnetic charge densities, can be written as

$$\tau_{z\alpha,\alpha} = 0; \quad D_{\alpha,\alpha} = 0; \quad B_{\alpha,\alpha} = 0, \quad \alpha = x, y \tag{4}$$

where $D_{\alpha,\alpha} = \partial D_x/\partial x + \partial D_y/\partial y$.
In view of Eqs. (1), (2), Eq. (4) can be reduced to

$$\mathbf{C}\left[\nabla^2 w, \nabla^2\varphi, \nabla^2\psi\right]^T = 0 \tag{5}$$

where $\nabla^2 = \partial^2/\partial x^2 + \partial^2/\partial y^2$ is the two-dimensional Laplace's operator.
Since $|\mathbf{C}| \neq 0$ one can decouple the system of governing equations (5)

$$\nabla^2 w = 0; \quad \nabla^2\varphi = 0; \quad \nabla^2\psi = 0 \tag{6}$$

3 Analysis

Consider an infinite magneto-electro-elastic medium containing an elliptical hole and boundary cracks emanating from it boundary. The hole and cracks are infinity extended in the direction of z- axis, which is the axis of polling. The $x0y$-plane is an isotropic plane. The medium subject to remote anti-plane stress τ_∞, in-plane electric displacement and magnetic induction D_∞ and B_∞ or electric field and magnetic field E_∞ and H_∞, as shown in Fig. 1 (two cases of electric and magnetic loads).

In order to formulate the boundary conditions, it is convenient to use a complex representation for w, φ and ψ which are grouped as a vector

$$\mathrm{Re}\,\mathbf{U}(z) = [w, \varphi, \psi]^T \tag{7}$$

where $z = x + \mathrm{i}y$, i is the imaginary unit, Re denotes the real part of a complex vector function $\mathbf{U}(z)$ and T denotes a transpose of a matrix.

The constitutive equations in complex form are expressed as follows:

$$\begin{Bmatrix} \tau_{xz} - \mathrm{i}\tau_{yz} \\ D_x - \mathrm{i}D_y \\ B_x - \mathrm{i}B_y \end{Bmatrix} = \begin{bmatrix} c_{44} & e_{15} & q_{15} \\ e_{15} & -\varepsilon_{11} & -d_{11} \\ q_{15} & -d_{11} & -\mu_{11} \end{bmatrix} \begin{bmatrix} \gamma_{xz} - \mathrm{i}\gamma_{yz} \\ -E_x + \mathrm{i}E_y \\ -H_x + \mathrm{i}H_y \end{bmatrix} = \mathbf{C}\mathbf{U}'(z) \tag{8}$$

where prime denotes the derivative with respect to z.

Since the stress, electric displacement and magnetic induction are divergence free in the absence of body force, electric and magnetic space charge densities, there exists the potential function $\mathbf{\Phi}(x, y)$, such that

$$[\tau_{xz}, D_x, B_x]^T = -\mathbf{\Phi}_{,y}, \quad [\tau_{yz}, D_y, B_y]^T = \mathbf{\Phi}_{,x} \tag{9}$$

where $\mathbf{\Phi}(z) = [\phi_1(z), \phi_2(z), \phi_3(z)]^T$ and comma denotes the differentiation with respect to x or y.

From Eqs. (8) and (9) we conclude that the complex potential functions $\mathbf{\Phi}(z)$ and $\mathbf{U}(z)$ are dependent as follows:

$$\mathbf{\Phi}(z) = \mathrm{i}\mathbf{C}\mathbf{U}(z) \tag{10}$$

If we take the integration of the traction t and normal electric displacement D_n and magnetic induction B_n as

$$\begin{Bmatrix} T_\tau \\ T_D \\ T_B \end{Bmatrix} = \int \begin{Bmatrix} t \\ D_\mathrm{n} \\ B_\mathrm{n} \end{Bmatrix} \mathrm{d}s = -\int \begin{Bmatrix} \tau_{yz}\mathrm{d}x - \tau_{xz}\mathrm{d}y \\ D_y\mathrm{d}x - D_x\mathrm{d}y \\ B_y\mathrm{d}x - B_x\mathrm{d}y \end{Bmatrix} = -\mathrm{Re}\int \mathrm{d}\mathbf{\Phi} = -\mathrm{Re}\,\mathbf{\Phi} = \mathrm{Im}[\mathbf{C}\mathbf{U}(z)] \tag{11}$$

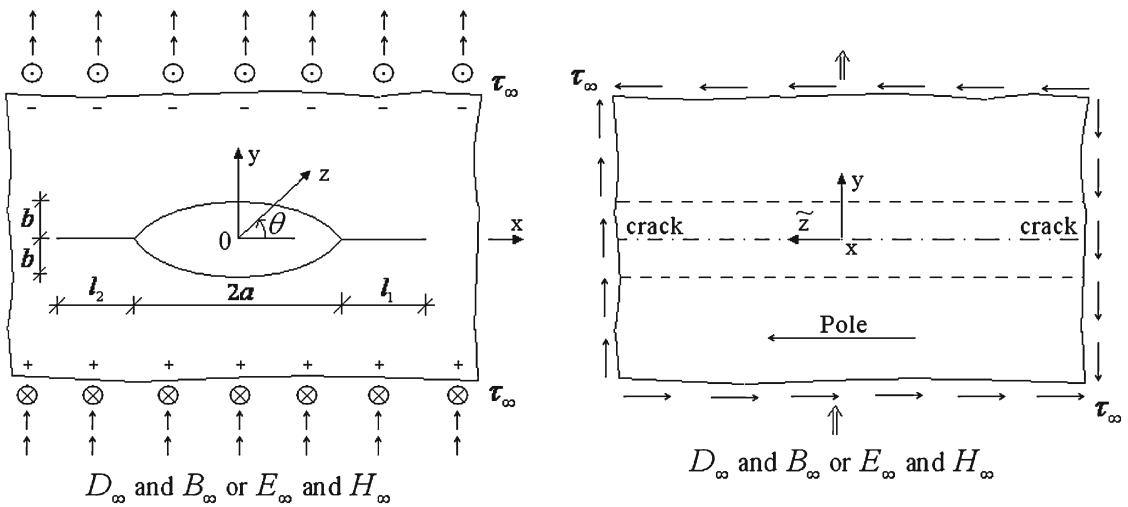

Fig. 1 Magneto-electro-elastic material with the elliptical hole and boundary cracks emanating from it boundary

then the mechanical, electric and magnetic boundary conditions along the surfaces of cracks and the elliptical hole can be formulated for vector function $\mathbf{\Phi}$.

The potential vector has the form

$$\mathbf{U}(z) = \mathbf{U}^{\infty} z + \mathbf{U}_0(z) \tag{12}$$

where $\mathbf{U}^{\infty}$ is a complex constant related to the loading condition at infinity and $\mathbf{U}_0(z)$ is an unknown complex function such that $\mathbf{U}_0(\infty) = 0$.

The complex constant $\mathbf{U}^{\infty}$ is defined as follows:

$$\mathbf{U}^{\infty} = \mathbf{C}^{-1} \begin{Bmatrix} \tau_{xz}^{\infty} - \mathrm{i}\tau_{yz}^{\infty} \\ D_x^{\infty} - \mathrm{i}D_y^{\infty} \\ B_x^{\infty} - \mathrm{i}B_y^{\infty} \end{Bmatrix} \tag{13}$$

for Case I boundary conditions (the superscript "-1" denotes the inverse of a matrix) and

$$\mathbf{U}^{\infty} = \begin{Bmatrix} \gamma_{xz}^{\infty} - \mathrm{i}\gamma_{yz}^{\infty} \\ -E_x^{\infty} + \mathrm{i}E_y^{\infty} \\ -H_x^{\infty} + \mathrm{i}H_y^{\infty} \end{Bmatrix} \tag{14}$$

for Case II boundary conditions.

The strains at infinity are

$$c_{44}\gamma_{xz}^{\infty} = \tau_{xz}^{\infty} + e_{15}E_x^{\infty} + q_{15}H_x^{\infty}, \quad c_{44}\gamma_{yz}^{\infty} = \tau_{yz}^{\infty} + e_{15}E_y^{\infty} + q_{15}H_y^{\infty} \tag{15}$$

In this study, two kinds of magneto-electric crack surface conditions are examined, i.e., magneto-electrically impermeable and permeable. For simplicity, they are identically expressed as

$$\tau_{yz} = 0, \quad D_y = d_0, \quad B_y = b_0 \quad \text{for elliptic hole and cracks.} \tag{16}$$

For the magneto-electrically impermeable case, both d_0 and b_0 vanish, whereas for the corresponding permeable case both d_0 and b_0 are unknown to be determined from the conditions

$$\varphi = 0, \quad \psi = 0 \quad \text{or} \quad U_2 = 0, \quad U_3 = 0 \quad \text{on surfaces of elliptic hole and cracks.} \tag{17}$$

On the plane $y = 0$ outside of the cracks the condition of anti-symmetry requires

$$\operatorname{Re}\mathbf{U}(z) = 0 \tag{18}$$

Impermeable boundary conditions occur when the dielectric permittivity and magnetic permeability of the void space inside the crack and hole (air or vacuum) are much smaller than those of the piezoelectromagnetic body.

Thus

$$\operatorname{Re}\mathbf{\Phi} = 0 \quad \text{or} \quad \mathrm{i}\mathbf{C}\mathbf{U}(z) + \overline{\mathrm{i}\mathbf{C}\mathbf{U}(z)} = 0 \quad \text{in the void space.} \tag{19}$$

Using the potential vector (12) we have

$$\mathrm{i}\mathbf{C}\mathbf{U}_0(z) + \overline{\mathrm{i}\mathbf{C}\mathbf{U}_0(z)} = -\left(\mathrm{i}\mathbf{C}\mathbf{U}^{\infty} + \overline{\mathrm{i}\mathbf{C}\mathbf{U}^{\infty}}\right) \quad \text{in the void space.} \tag{20}$$

3.1 Conforming mapping

Consider of conformal mapping function

$$z = \omega(\varsigma) = \frac{a\mu(\varsigma) + b\sqrt{\mu^2(\varsigma) - 16\varsigma^2}}{4\varsigma} \tag{21}$$

where

$$\mu(\varsigma) = \varepsilon_1(1+\varsigma)^2 + \varepsilon_2(1-\varsigma)^2 \tag{22}$$

These equations provide a conformal mapping from domain of material, which occupies the outside region of the elliptical hole and cracks in the z-plane, to the interior of a unit circle in the ς-plane (Fig. 2).

The parameters ε_1 and ε_2 are obtained from equations

$$(-1)^{i-1}(a + l_i) = \omega[(-1)^{i-1}], \quad \text{i.e.,} \quad a + l_i = a\varepsilon_i + b\sqrt{\varepsilon_i^2 - 1}, \quad i = 1, 2 \tag{23}$$

and are

$$\varepsilon_i = \left[a(l_i + a) - b\sqrt{l_i^2 + 2al_i + b^2}\right] / \left(a^2 - b^2\right) \tag{24}$$

In the special cases ε_i are obtained as follows:

(i) $\varepsilon_i = \frac{1}{2}\left(1 + \lambda_i + \frac{1}{1+\lambda_i}\right)$, for circular hole and two edge cracks, $\lambda_i = l_i/a$
(ii) $\varepsilon_i = 1 + \lambda_i$, for line crack ($b \to 0$) of length $2a + l_1 + l_2 = a(\varepsilon_1 + \varepsilon_2)$
(iii) $b\varepsilon_i = \sqrt{l_i^2 + b^2}$, for the cross-shaped crack ($a \to 0$)

In the ς-plane Eq. (19) can be rewritten as

$$\mathrm{i}\mathbf{C}\mathbf{U}_0(\sigma) + \overline{\mathrm{i}\mathbf{C}\mathbf{U}_0}(\sigma) = -\left(\mathrm{i}\mathbf{C}\mathbf{U}^{\infty}\omega(\sigma) + \overline{\mathrm{i}\mathbf{C}\mathbf{U}}^{\infty}\overline{\omega}(\sigma)\right) \tag{25}$$

in which σ is the point on the unit circle and $\mathbf{U}_0(\sigma) = \mathbf{U}_0[\omega(\sigma)]$ is defined. It is clarified that $\overline{\omega}(\sigma) = \omega(\sigma)$ as show Eq. (21).

Therefore Eq. (25) becomes

$$\mathrm{i}\mathbf{C}\mathbf{U}_0(\sigma) + \overline{\mathrm{i}\mathbf{C}\mathbf{U}_0}(\sigma) = -\mathbf{\Phi}^{\infty}_{,x}\omega(\sigma) \tag{26}$$

where Eqs. (10) and (12) are used

Taking Cauchy integral

$$\frac{1}{2\pi\mathrm{i}}\int_{\gamma}\frac{(\,)}{\sigma - \varsigma}\mathrm{d}\sigma \tag{27}$$

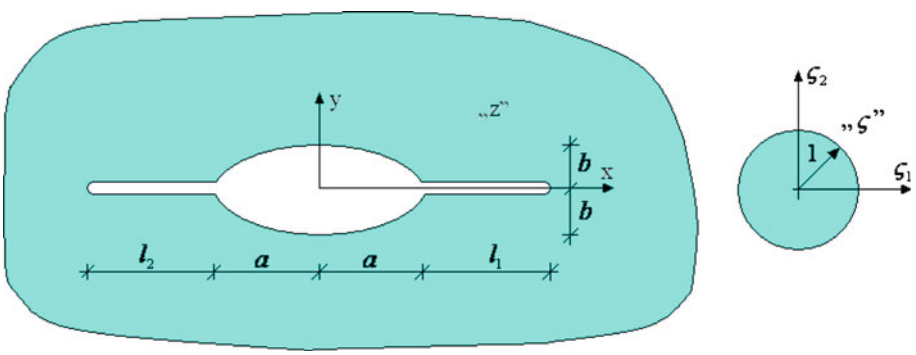

Fig. 2 The conformal mapping from z-plane to ς-plane

at the two sides of Eq. (25) gives

$$\mathbf{iCU}_0(\varsigma) = -\mathbf{\Phi}_{,x}^{\infty}\frac{1}{2\pi i}\int\limits_{\gamma}\frac{\omega(\sigma)}{\sigma-\varsigma}\mathrm{d}\sigma, \quad |\varsigma|<1 \tag{28}$$

In this calculation the condition that $\mathbf{iCU}_0(\varsigma)$ is analytic in the interior of a unit circle γ is used.

Since $\omega(\sigma)$ is the boundary value of the analytic function $\omega(\varsigma)$ inside the unit circle γ except to the point $\varsigma = 0$, we obtain from Eq. (28) [7]

$$\mathbf{iCU}_0(\varsigma) = -\mathbf{\Phi}_{,x}^{\infty}\omega_s(\varsigma) \tag{29}$$

where $\omega_s(\varsigma)$ is the singular part of $\omega(\varsigma)$ at the point $\varsigma = 0$. It is

$$\omega_s(\varsigma) = \frac{(a+b)(\varepsilon_1+\varepsilon_2)}{4\varsigma} \tag{30}$$

Thus

$$\mathbf{iCU}_0(\varsigma) = -\mathbf{\Phi}_{,x}^{\infty}\frac{(a+b)(\varepsilon_1+\varepsilon_2)}{4\varsigma} \tag{31}$$

Differentiating this equation with respect to ς and using that $\mathbf{U}_0(\varsigma) = \mathbf{U}_0[\omega(\varsigma)]$, we obtain

$$\omega'(\varsigma)\mathbf{\Phi}_{,x}(\varsigma) = \mathbf{\Phi}_{,x}^{\infty}\frac{(a+b)(\varepsilon_1+\varepsilon_2)}{4\varsigma^2} \tag{32}$$

where

$$\omega'(\varsigma) = -\frac{\left(1-\varsigma^2\right)(\varepsilon_1+\varepsilon_2)}{4\varsigma^2}\left(a+b\frac{\mu(\varsigma)}{\sqrt{\mu^2(\varsigma)-16\varsigma^2}}\right) \tag{33}$$

Thus

$$\begin{Bmatrix}\tau_{yz}\\ D_y\\ B_y\end{Bmatrix} = \begin{Bmatrix}\tau_{yz}^{\infty}\\ D_y^*\\ B_y^*\end{Bmatrix}\frac{(a+b)(\varepsilon_1+\varepsilon_2)}{4\varsigma^2\omega'(\varsigma)} \tag{34}$$

where

$$\begin{aligned} D_y^* &= \begin{cases} D_y^{\infty}, & \text{Case I}\\ \frac{e_{15}}{c_{44}}\tau_{yz}^{\infty} + \left(\varepsilon_{11}+\frac{e_{15}^2}{c_{44}}\right)E_y^{\infty} + \left(d_{11}+\frac{q_{15}e_{15}}{c_{44}}\right)H_y^{\infty}, & \text{Case II}\end{cases}\\ B_y^* &= \begin{cases} B_y^{\infty}, & \text{Case I}\\ \frac{q_{15}}{c_{44}}\tau_{yz}^{\infty} + \left(d_{11}+\frac{e_{15}q_{15}}{c_{44}}\right)E_y^{\infty} + \left(\mu_{11}+\frac{q_{15}^2}{c_{44}}\right)H_y^{\infty}, & \text{Case II}\end{cases}\end{aligned} \tag{35}$$

The field intensity factors in the ς-plane are defined as follows:

$$\begin{Bmatrix}k_{\tau i}\\ k_{Di}\\ k_{Bi}\end{Bmatrix} = \lim_{\varsigma\to\pm1}\sqrt{2\pi|\omega(\varsigma)-\omega(\pm1)|}\begin{Bmatrix}\tau_{yz}\\ D_y\\ B_y\end{Bmatrix} \tag{36}$$

we obtain

$$\begin{Bmatrix}k_{\tau i}\\ k_{Di}\\ k_{Bi}\end{Bmatrix} = \begin{Bmatrix}\tau_{yz}^{\infty}\\ D_y^*\\ B_y^*\end{Bmatrix}\sqrt{\frac{\pi}{2}}(a+b)(\varepsilon_1+\varepsilon_2)\lim_{\varsigma\to\pm1}\frac{\sqrt{|\omega(\varsigma)-\omega(\pm1)|}}{\omega'(\varsigma)} \tag{37}$$

Since $\omega'(\pm 1) = 0$ we use the l'Hospital rule to obtain

$$\lim_{\varsigma \to \pm 1} \sqrt{\frac{|\omega(\varsigma) - \omega(\pm 1)|}{[\omega'(\varsigma)]^2}} = \frac{1}{\sqrt{2|\omega''(\pm 1)|}} \tag{38}$$

where

$$\begin{aligned} \omega''(\varsigma) &= \frac{\varepsilon_1 + \varepsilon_2}{2\varsigma^3}\left(a + b\frac{\mu(\varsigma)}{\sqrt{\mu^2(\varsigma) - 16\varsigma^2}}\right) - \frac{4\left(1-\varsigma^2\right)^2(\varepsilon_1+\varepsilon_2)^2 b}{\varsigma}\frac{1}{\left(\mu^2(\varsigma) - 16\varsigma^2\right)^{3/2}} \\ \omega''\left((-1)^{i-1}\right) &= (-1)^{i-1}\frac{\varepsilon_1+\varepsilon_2}{2}\left(a + b\frac{\varepsilon_i}{\sqrt{\varepsilon_1^2 - 1}}\right); \quad i = 1, 2 \end{aligned} \tag{39}$$

The stress, electric displacement and magnetic induction intensity factors are obtained as follows:

$$\left\{\begin{matrix} \text{SIFs} \\ \text{EDIFs} \\ \text{MIIFs} \end{matrix}\right\}^{\text{imp.}} : \left\{\begin{matrix} k_{\tau i} \\ k_{Di} \\ k_{Bi} \end{matrix}\right\} = \sqrt{\frac{\pi}{2}(l_1 + l_2)} \left\{\begin{matrix} \tau_{yz}^{\infty} \\ D_y^* \\ B_y^* \end{matrix}\right\} K_i \tag{40}$$

where K_i is the coefficient of field intensity factors defined by equation

$$K_i = \frac{1+\lambda}{\sqrt{\lambda_1 + \lambda_2}}\sqrt{\frac{\varepsilon_1 + \varepsilon_2}{1 + \lambda\varepsilon_i/\sqrt{\varepsilon_i^2 - 1}}}, \quad i = 1, 2; \quad \lambda = b/a \tag{41}$$

In the special cases K_i approaches the values:

(i)

$$K_i = \sqrt{\frac{\lambda_i}{1+\lambda_i}\left(1 + \frac{1}{1+\lambda_i}\right)\left(1 + \frac{2}{\lambda_1+\lambda_2}\right)\left(1 + \frac{1}{(1+\lambda_1)(1+\lambda_2)}\right)}, \quad \lambda_i = \frac{l_i}{a} \tag{42}$$

for circular hole and two asymmetrical edge cracks

(ii)

$$K_i = \sqrt{1 + \frac{2}{\lambda_1 + \lambda_2}} \tag{43}$$

for line crack of length $2a + l_1 + l_2$, $\lambda \equiv 0$

(iii)

$$K_i = \sqrt{\frac{\lambda_i}{\lambda_1+\lambda_2}\frac{\sqrt{\lambda_1^2+1} + \sqrt{\lambda_2^2+1}}{\sqrt{\lambda_i^2+1}}} \tag{44}$$

for the asymmetrical cross-shaped crack, $\lambda_i = l_i/b$, $a \to 0$

The classical result, for $K_i \equiv 1$, is obtained in three cases, namely, for line crack of length $l_1 + l_2$, the symmetrical cross-shaped crack and edge crack. In all of these cases the stress τ_{xz} is zero on the plane $x = 0$, since it is the plane of symmetry in these cases.

When the left crack length l_2 tends to zero ($\varepsilon_2 = 1$) K_1 is

$$K_i = \frac{1+\lambda}{\sqrt{\lambda_1}}\sqrt{\frac{1+\varepsilon_1}{1 + \lambda\varepsilon_1/\sqrt{\varepsilon_1^2 - 1}}} \tag{45}$$

This is the solution for a single crack emanating from an elliptical hole. This result coincides with the one obtained by [12,20] in the framework of linear theory of elasticity.

When the piezoelectric, piezomagnetic and magneto-electric constants are ignored, the above results can be reduced to these presented by [11]. When the piezomagnetic and magneto-electric effect are omitted, the results obtained here are reduced to presented by [3].

From Eq. (40) it is easy known that the SIFs, the EDIFs and the MIIFs are independent and that they are only related to the corresponding mechanical, electrical and magnetical loading for fully impermeable crack boundary conditions.

So that it should be notched that for magneto-electro-elastically impermeable cracks as electrical and/or magnetical load are applied, the SIFs cannot perfectly describe the fracture characteristics as in the purely elastic case.

Therefore, the energy release rates (ERRs) are introduced by calculating the work done in closing the crack tip over an infinitesimal distance. The energy release rate is derived in the following in a similar manner to proposed by [10] and also utilized by [1,17].The energy release rate G at the crack-tip is obtained from the following integral:

$$G = \frac{1}{2}\lim_{\delta\to 0}\frac{1}{\delta}\int_0^{\delta}\left\{\tau_{yz}(r+a,0)\Delta w(r+a-\delta) + D_y(r+a,0)\Delta\varphi(r+a-\delta) + B_y(r+a,0)\Delta\psi(r+a-\delta)\right\}\mathrm{d}r \tag{46}$$

where Δw, $\Delta\varphi$ and $\Delta\psi$ are the jumps of displacement, electric potential and magnetic potential. These jumps define the displacement, electric potential and magnetic potential field intensity factors $\tilde{k}_w$, $\tilde{k}_\varphi$ and $\tilde{k}_\psi$ as the respective limits for $\delta \to 0$.

Then, the energy release rate, defined by (46), may be written as

$$G = \frac{1}{2}\left(k_\tau\tilde{k}_w + k_D\tilde{k}_\varphi + k_B\tilde{k}_\psi\right) \tag{47}$$

The field intensity factors $\tilde{k}_w$, $\tilde{k}_\varphi$ and $\tilde{k}_\psi$ may be calculated from constitutive equations which, in matrix form and explicit form, may be written as follows:

$$\begin{aligned}
\left[\tilde{k}_w,\,\tilde{k}_\varphi,\,\tilde{k}_\psi\right]^T &= \mathbf{C}^{-1}\left[k_\tau,\,k_D,\,k_B\right]^T\\
\tilde{k}_w &= \frac{\varepsilon_{11}\mu_{11}-d_{11}^2}{\Delta}k_\tau + \frac{e_{15}\mu_{11}-q_{15}d_{11}}{\Delta}k_D + \frac{q_{15}\varepsilon_{11}-e_{15}d_{11}}{\Delta}k_B\\
\tilde{k}_\varphi &= \frac{e_{15}\mu_{11}-q_{15}d_{11}}{\Delta}k_\tau - \frac{c_{44}\mu_{11}+q_{15}^2}{\Delta}k_D + \frac{c_{44}d_{11}+e_{15}q_{15}}{\Delta}k_B\\
\tilde{k}_\psi &= \frac{q_{15}\varepsilon_{11}-e_{15}d_{11}}{\Delta}k_\tau + \frac{c_{44}d_{11}+e_{15}q_{15}}{\Delta}k_D - \frac{c_{44}\varepsilon_{11}+e_{15}^2}{\Delta}k_B
\end{aligned} \tag{48}$$

The ERR, G, is obtained, in matrix notation and explicit formula, as follows:

$$\begin{aligned}
G &= \frac{1}{2}[k_\tau,k_D,k_B]\mathbf{C}^{-1}[k_\tau,k_D,k_B]^T\\
G_i &= \frac{\pi}{4}(l_1+l_2)K_i^2\left(\frac{\varepsilon_{11}\mu_{11}-d_{11}^2}{\Delta}\tau_{yz}^{\infty 2} - \frac{c_{44}\mu_{11}+q_{15}^2}{\Delta}D_y^{*2} - \frac{c_{44}\varepsilon_{11}+e_{15}^2}{\Delta}B_y^{*2}\right.\\
&\quad \left. +2\frac{e_{15}\mu_{11}-q_{15}d_{11}}{\Delta}\tau_{yz}^{\infty}D_y^* + 2\frac{q_{15}\varepsilon_{11}-e_{15}d_{11}}{\Delta}\tau_{yz}^{\infty}B_y^* + 2\frac{c_{44}d_{11}+e_{15}q_{15}}{\Delta}D_y^*B_y^*\right)
\end{aligned} \tag{49}$$

where

$$\Delta = c_{44}\varepsilon_{11}\mu_{11} - c_{44}d_{11}^2 + e_{15}^2\mu_{11} - 2e_{15}q_{15}d_{11} + q_{15}^2\varepsilon_{11} \tag{50}$$

The ERRs of special cases of crack can be calculated by using Eq. (49) and by substituting the coefficient of fields intensity factors K_i from Eqs. (42)–(44).

3.2 Magneto-electrically permeable cracks

From boundary conditions (17) we obtain

$$d_0 = \begin{cases} D_y^\infty - \frac{e_{15}}{c_{44}}\tau_{yz}^\infty, & \text{Case I} \\ \left(\varepsilon_{11} + \frac{e_{15}^2}{c_{44}}\right) E_y^\infty + \left(d_{11} + \frac{q_{15}e_{15}}{c_{44}}\right) H_y^\infty, & \text{Case II} \end{cases}$$
$$b_0 = \begin{cases} B_y^\infty - \frac{q_{15}}{c_{44}}\tau_{yz}^\infty, & \text{Case I} \\ \left(d_{11} + \frac{e_{15}q_{15}}{c_{44}}\right) E_y^\infty + \left(\mu_{11} + \frac{q_{15}^2}{c_{44}}\right) H_y^\infty, & \text{Case II} \end{cases} \tag{51}$$

Then, using Eq. (35), we obtain

$$\begin{aligned} D_y^* - d_0 &= \frac{e_{15}}{c_{44}}\tau_{yz}^\infty \\ B_y^* - b_0 &= \frac{q_{15}}{c_{44}}\tau_{yz}^\infty \end{aligned} \tag{52}$$

in both cases of loading conditions.

The mode III stress/electric/magnetic intensity factors (the singularities are proportional to τ_{yz}^∞, $D_y^* - d_0$ and $B_y^* - b_0$, respectively) are obtained as follows:

$$\begin{aligned} k_{\tau i} &= \sqrt{\frac{\pi}{2}(l_1 + l_2)}\tau_{yz}^\infty K_i \\ k_{Di} &= \frac{e_{15}}{c_{44}} k_{\tau i} \\ k_{Bi} &= \frac{q_{15}}{c_{44}} k_{\tau i} \end{aligned} \tag{53}$$

The energy release rate is

$$G_i = \frac{\pi}{4}(l_1 + l_2)\frac{\left(\tau_{yz}^\infty\right)^2}{c_{44}} K_i^2 \tag{54}$$

and is obtained from formulae (47)–(49) by substitution the solution (53) for permeable case.

Equation (53) indicates that the three field intensity factors stress, electric displacement and magnetic induction are dependent on each other through material constants.

In addition, $k_{\tau i}$ depends only on τ_{yz}^∞ and both d_0 and b_0 have no effects on these field intensity factors.

4 Numerical results and discussions

In order to have better understanding for the theoretical results above, numerical computations are given to illustrate the effect of variable geometrical and material parameters on stress, electric and magnetic intensity factors and energy release rate.

Computations for the energy release rate have been caried out to illustrate the magneto-electro-elastic coupled behaviour of a $BaTiO_3 - CoFe_2O_4$ composite material with a volume fraction $V_f = 0.5$. Material constants are listed in Table 1 [13].

The investigation of the ERRs, G_i, defined by Eq. (49) gives some conclusions, which are shown in Fig. 3.

Figures 4 and 5 show the variation of the coefficient of field intensity factors K_1. The field intensity factors for a single crack are smaller than those of two cracks originating from a circular (Fig. 4) or an elliptical hole, since k_i is given by Eq. (40). Although, the K_i increases as λ_2 decreases, but the multiplier of K_i in Eq. (40) depends on $\sqrt{l_1 + l_2}$ and increases with l_2.

Figure 6 shows the variation of ERRs for impermeable crack versus τ_{yz}^∞ for circular hole and two equal edge cracks with $l/a = 0.5; 1.0; 2.0$. The ERRs increases with increasing of l/a.

Table 1 Material properties of single-phase materials and composite

	$BaTiO_3$ piezoelectric	$CoFe_2O_4$ piezoelectric	$BaTiO_3 - CoFe_2O_4$ (composite, $V_f = 0.5$)
c_{44}(GPa)	43	45	44
e_{15}(C/m^2)	11.6	0	5.8
q_{15}(N/Am)	0	550	275
ε_{11}(nC/Vm)	11.2	0.08	5.64
d_{11}(nC/Am)	10	0.8	5.4
$\mu_{11}(\mu$N/A$^2)$	5	589	297

n, nano $= 10^{-9}$; μ, mikro $= 10^{-6}$; G, giga $= 10^9$

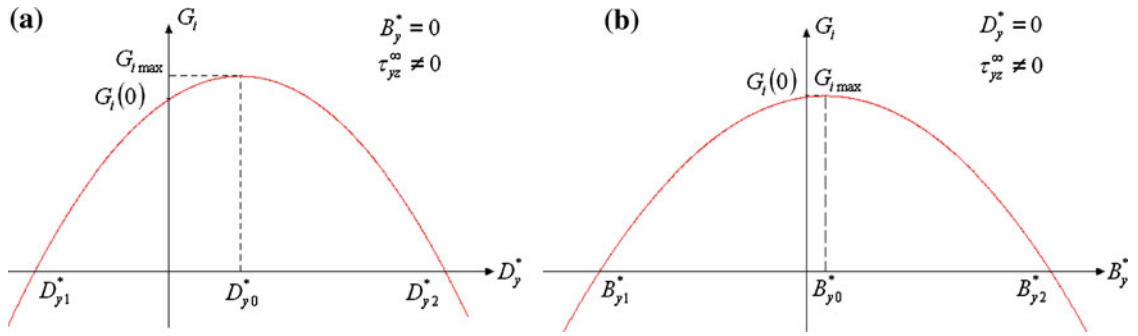

Fig. 3 Effects of applied electric load D_y^* (**a**) and magnetic load B_y^* (**b**) on the energy release rate G_i at a given mechanical load τ_{yz}^∞, $\left(D_{y1}^*, D_{y0}^*, D_{y2}^*\right) \equiv (-2,492;\ 1,311;\ 5,114) \cdot 10^{-10}\tau_{yz}^\infty$, $G_{i\,\max} = 2.260 \cdot 10^{-11}(\pi/4)(l_1 + l_2)K_i^2(\tau_{yz})^2$, $G_i(0) = 0.881\ G_{i\,\max}$ and $\left(B_{y1}^*, B_{y0}^*, B_{y2}^*\right) \equiv (-7{,}179;\ 0{,}550;\ 8{,}280)\cdot 10^{-10}\tau_{yz}^\infty$, $G_{i\,\max} = 2.001\cdot 10^{-11}(\pi/4)(l_1 + l_2)K_i^2(\tau_{yz})^2$, $G_i(0) = 0.995\ G_{i\,\max}$

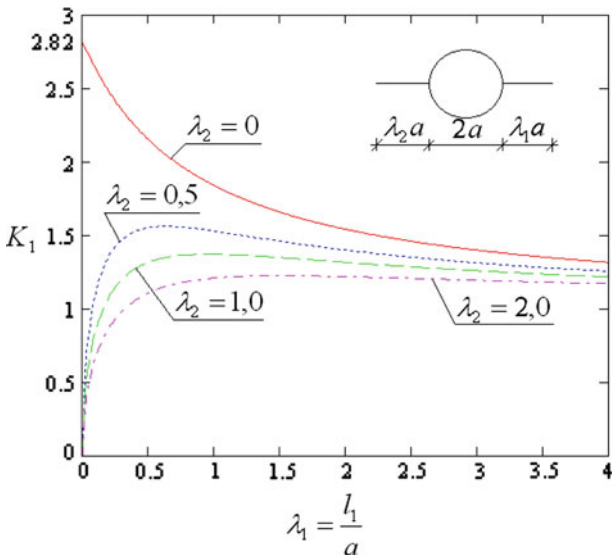

Fig. 4 Variation of K_1 with a ratio λ_1

Figures 7 and 8 present result of ERRs [Eqs. (49) with (35) for impermeable crack and Eq. (54) for permeable crack] with respect to $10\tau_{yz}^\infty\tau^{-1}(\tau = 10\,\text{MPa})$, τ_{yz}^∞ varying from 0.02τ to 0.2τ, $0.2 \le \tau_{yz}^\infty \le 2.0$, for $D = 0.001\,\text{C/m}^2$, $B = 0.1\,\text{N/Am}$ in Case I and for $E = 1\,\text{kV/cm}$, $H = 1\,\text{kA/m}$ in Case II of boundary conditions.

The variations of the electric displacement d_0 and magnetic induction b_0 inside the crack on the applied mechanical loads are drawn in Fig. 9 under applied electrical displacements $D_y^\infty = 0.1D$ or $0.12D$ and

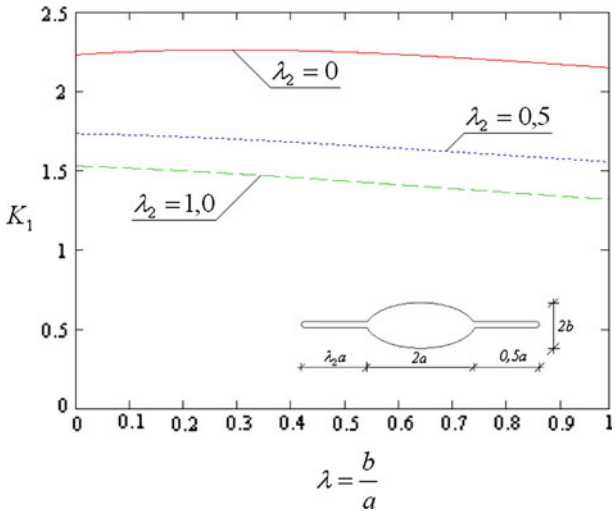

Fig. 5 Variation of K_1 with a ratio λ

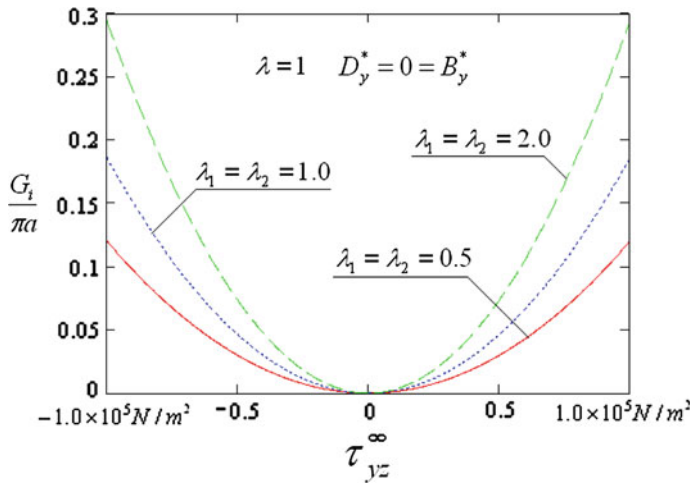

Fig. 6 ERRs versus τ_{yz}^{∞} for $D_y^* = 0 = B_y^*$ (impermeable crack)

magnetic inductions $B_y^{\infty} = 0.1B$ or $0.12B$, where $D = 0.001\,\mathrm{C/m^2}$ and $B = 0.1\,\mathrm{N/Am}$. The values of d_0 and b_0 decrease from positive to negative values with increasing the mechanical loading (Fig. 9).

The variations of d_0 and b_0 inside the crack on the applied mechanical loads are drawn in Fig. 10 under applied electrical field $E_y^{\infty} = 0.1E$ or $0.12E$ and magnetic field $H_y^{\infty} = 0.1H$ or $0.12H$, where $E = 1\,\mathrm{kV/cm}$ and $H = 1\,\mathrm{kA/m}$.

It is seen from Fig. 10 that the values of d_0 and b_0 are independent of mechanical loads and are higher for larger electrical and magnetic field.

5 Conclusions

From the analytical or numerical results, several conclusions can be obtained:

- For the magneto-electrically impermeable cracks, the SIFs, the EDIFs and MIIFs are related to applied loads, respectively, mechanical, electrical and magnetical only. The ERRs depend on both applied loads including mechanical, electrical and magnetical and material parameters. For the magneto-electrically permeable cracks, both electrical and magnetical loads have no contribution to ERRs and field intensity factors. Those physical quantities depend on the level of the applied mechanical load and on the material parameters. The value of ERRs for magneto-electrically permeable crack is higher than that impermeable

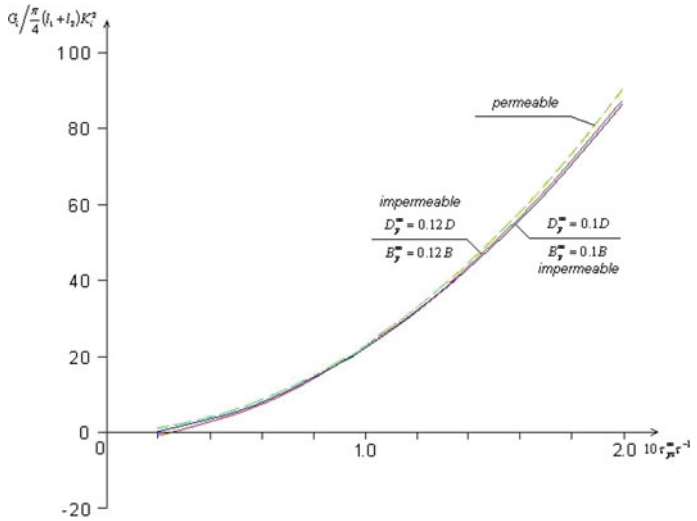

Fig. 7 The variation of ERRs (N/m) obtained with respect to $10\,\tau_{yz}^{\infty}\tau^{-1}(\tau = 10\,\text{MPa})$, $D = 0.001\,\text{C/m}^2$, $B = 0.1\,\text{N/Am}$ in impermeable and permeable crack boundary conditions $\left[G_i/\frac{\pi}{4}(l_1 + l_2)K_i^2\right]$

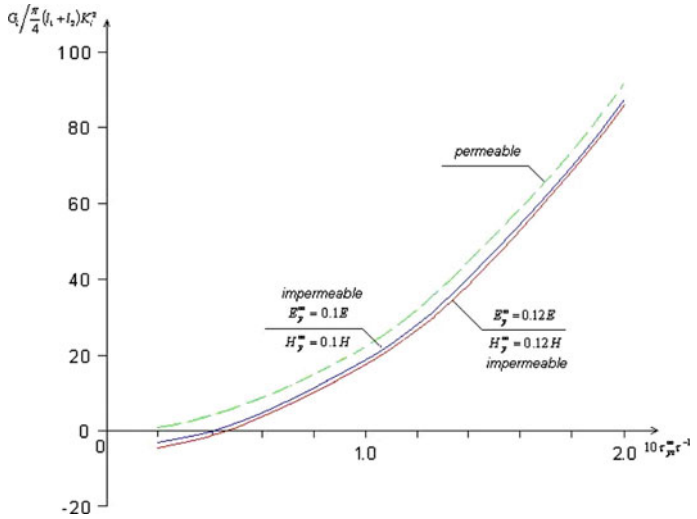

Fig. 8 The variation of ERRs (N/m) obtained with respect to $10\,\tau_{yz}^{\infty}\tau^{-1}(\tau = 10\,\text{MPa})$, $E = 1\,\text{kV/cm}$, $H = 1\,\text{kA/m}$ in impermeable and permeable crack boundary conditions $\left[G_i/\frac{\pi}{4}(l_1 + l_2)K_i^2\right]$

case under only mechanical loading. The effect of magnetic permeability of air (or vacuum) inside the crack is more significant than the electric permittivity. Therefore, neglecting the magnetic permeability of the medium inside the crack will have more significant consequence on ERRs than neglecting the electric permeability.

- For given mechanical load, the negative electric or/and magnetic field(s), usually retard(s) crack growth while the positive electrical or/and magnetic field(s) can either promote(s) or retard(s) crack propagation, which is depended on both strengths of the applied electric or/and magnetic field(s) and the level of the mechanical load. The directions of separately applied D_y^* and B_y^* do not affect the value of maximum ERRs while the directions of simultaneously applied D_y^* and B_y^* do. Negative values of ERRs are physically impossible. This observation implies that a pure electromagnetic loading $\left(D_y^*, B_y^*\right)$ would be expected to retard the propagation of the crack in PEMO-elastic material. For a given mechanical loading there is a pair of D_y^* or/and B_y^* which makes the G_i to maximum.

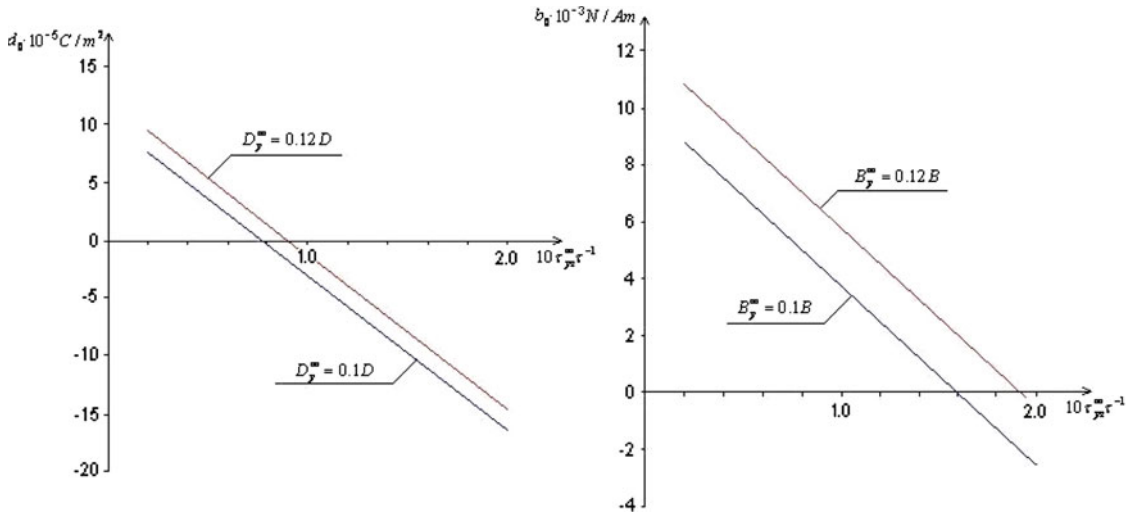

Fig. 9 The variation of d_0 and b_0 on $10\,\tau_{yz}^{\infty}\tau^{-1}(\tau = 10\,\text{MPa})$ with $D = 0.001\,\text{C/m}^2$, $B = 0.1\,\text{N/Am}$ for $D_y^{\infty} = 0.1D$, $B_y^{\infty} = 0.1B$ and $D_y^{\infty} = 0.12D$, $B_y^{\infty} = 0.12B$, respectively.

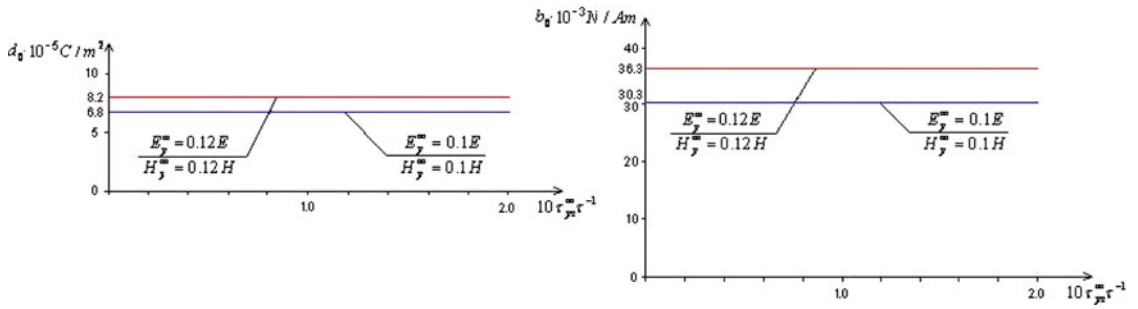

Fig. 10 The variation of d_0 and b_0 on $10\,\tau_{yz}^{\infty}\tau^{-1}(\tau = 10\,\text{MPa})$ with $E = 1\,\text{kV/cm}$, $H = 1\,\text{kA/m}$ for $E_y^{\infty} = 0.1E$, $H_y^{\infty} = 0.1H$ and $E_y^{\infty} = 0.12E$, $H_y^{\infty} = 0.12H$, respectively.

The next observation is that, even in the case of pure mechanical load, the energy release rates for the fully permeable crack and the fully impermeable crack are different and the G_i for permeable crack is about 14% higher than that for impermeable case.

The above conclusions could have applications in the failure of piezo-electro-magneto-elastic devices and in smart materials/intelligent structures.

References

1. Feng, W.J., Su, R.K.L.: Dynamic internal crack problem of a functionally graded magneto-electro-elastic strip. Int. J. Solids Struct. **43**, 5196–5216 (2006)
2. Gao, C.F., Tong, P., Zhang, T.Y.: Fracture mechanics for a mode III crack in a magnetoelectroelastic solid. Int. J. Solids Struct. **41**, 6613–6629 (2004)
3. Guo, J.H., Lu, Z.X., Han, H.T., Yang, Z.: Exact solution for anti-plane problem of two axisymmetrical edge cracks emanating from an elliptical hole in a piezoelectric material. Int. J. Solids Struct. **46**, 3799–3809 (2009)
4. Hu, K.Q., Zhong, Z., Jin, B.: Anti-plane shear crack in a functionally gradient piezoelectric layer boded to dissimilar half spaces. Int. J. Mech. Sci. **47**, 82–93 (2005)
5. Hu, K.Q., Qin, Q.H., Kang, Y.L.: Anti-plane shear crack in a magnetoelectroelastic layer sandwiched between dissimilar half spaces. Eng. Fract. Mech. **74**, 1139–1147 (2007)
6. Li, R., Kardomateas, G.A.: The mode III interface crack in piezo-electro-magneto-elastic dissimilar bimaterials. Trans. ASME J. Appl. Mech. **73**, 220–227 (2006)
7. Ma, L., Li, J., Abdelmoula, R., Wu, L.Z.: Mode III crack problem in a functionally graded magneto-electro-elastic strip. Int. J. Solids Struct. **44**, 5518–5537 (2007)
8. Muskhelishvili, N.L.: Some Basic Problems of Mathematical Theory of Elasticity. Noordhoff, Leyden (1975)

9. Ou, Y.L., Chue, C.H.: Two mode III internal cracks located within two bonded functionally graded piezoelectric half planes respectively. Arch. Appl. Mech. **75**, 364–378 (2006)
10. Pak, Y.E.: Crack extension force in a piezoelectric material. Trans. ASME J. Appl. Mech. **57**, 647–653 (1990)
11. Sih, G.C.: Stress-intensity factors for longitudinal shear cracks. AIAA J. **1**(10), 2387–2388 (1963)
12. Sih, G.C.: Stress distribution near internal crack tips for longitudinal shear problems. Trans. ASME J. Appl. Mech. **32**, 51–58 (1965)
13. Song, Z.F., Sih, G.C.: Crack initation behavior in magnetoelectroelastic composite under in-plane deformation. J. Theor. Appl. Fract. Mech. **39**, 189–207 (2003)
14. Su, R.K.L., Feng, W.J., Liu, J.: Transient response of interface cracks between dissimilar magneto-electro-elastic strips under out-of-plane mechanical and in-plane magneto-electrical impact loads. Compos. Struct. **78**, 119–128 (2007)
15. Wang, B.L., Han, J.C., Mai, Y.W.: Mode III fracture of a magnetoelectroelastic layer: exact solution and discussion of the crack face electromagnetic boundary conditions. Int. J. Frac. **139**, 27–38 (2006)
16. Wang, B.L., Mai, Y.W.: Closed-form solution for an antiplane interface crack between two dissimilar magnetoelectroelastic layers. Trans. ASME J. Appl. Mech. **73**, 281–290 (2006)
17. Wang, X.Y., Yu, S.W.: Transient response for a crack in a piezoelectric strip subjected to the mechanical and electrical impact: mode III problem. Int. J. Solid Struct. **37**, 5795–5808 (2000)
18. Wang, Y.J., Gao, C.F.: The mode III cracks originating from the edge of a circular hole in a piezoelectric solid. Int. J. Solid Struct. **45**, 4590–4599 (2008)
19. Yang, F., Kao, I.: Crack problem in piezoelectric materials: general anti-plane mechanical loading. Mech. Mater. **31**, 309–406 (1999)
20. Yokobori, T., Kamei, A., Konosu, S.: The stress intensity factors for an elliptical notch with two collinear cracks at its tips. Rep. Res. Inst. Strength Fract. Mater. Tohoku Univ. **7**(2), 57–62 (1971)
21. Zhang, T.Y., Hack, J.E.: Mode-III crack in piezoelectric materials. J. Appl. Phys. **71**, 5865–5870 (1992)
22. Zhang, T.Y., Tong, P.: Fracture mechanics for mode III crack in a piezoelectric material. Int. J. Solid Struct. **33**, 343–353 (1996)
23. Zhang, T.Y., Qian, C.F., Tong, P.: Linear electro-elastic analysis of a cavity or a crack in piezoelectric material. Int. J. Solid Struct. **35**, 2121–2149 (1998)
24. Zhou, Z.G., Wu, L.Z., Wang, B.: The behaviour of a crack in functionally graded piezoelectric/piezomagnetic materials under anti-plane shear loading. Arch. Appl. Mech. **74**, 526–535 (2005)